



## Adsorption of methylene blue and methyl violet by camellia seed powder: kinetic and thermodynamic studies

Chongchen Wang<sup>a,c,\*</sup>, Jia Zhang<sup>b</sup>, Peng Wang<sup>a</sup>, Hao Wang<sup>c</sup>, Hui Yan<sup>c</sup>

<sup>a</sup>Key Laboratory of Urban Stormwater System and Water Environment (Ministry of Education), Beijing University of Civil Engineering and Architecture, Beijing 100044, China

Tel. +86 10 68322124; Fax: +86 10 6832 2128; email: [chongchenwang@126.com](mailto:chongchenwang@126.com)

<sup>b</sup>Beijing Climate Change Response Research and Education Center, Beijing University of Civil Engineering and Architecture, Beijing 100044, China

<sup>c</sup>The College of Materials Science and Engineering, Beijing University of Technology, Beijing 100022, China

Received 9 October 2013; Accepted 27 November 2013

---

### ABSTRACT

Adsorption of methylene blue (MB) and methyl violet (MV) onto camellia seed powder (CSP) was conducted, and the equilibrium data were fitted with Langmuir, Freundlich and Dubinin–Radushkevich (D–R) models to describe the equilibrium isotherms. The kinetics rates were modeled using pseudo-first-order, pseudo-second-order kinetic equations, and intra-particle diffusion model. The results revealed that adsorption of MB and MV onto CSP was affected slightly by the pH value, and the maximum adsorption amount was achieved at the pH of 5.5, the unadjusted value. For MB, the adsorption process could be depicted primarily by Langmuir function, while for MV, the equilibrium data agree well with all of the Langmuir, Freundlich, and D–R models. The Gibbs free energy ( $\Delta G^0$ ), enthalpy change ( $\Delta H^0$ ), and entropy change ( $\Delta S^0$ ) for MB were all below zero, which indicated the adsorption was spontaneous and exothermic process; while for MV, the negative  $\Delta G^0$  value and positive  $\Delta H^0$  value imply that its adsorption process is spontaneous and endothermic. For both MB and MV, the kinetics data were better fitted with the pseudo-second-order kinetic model and the intra-particle diffusion controls the adsorption rate.

*Keywords:* Camellia seed powder; Dye; Adsorption; Thermodynamics; Kinetics

---

### 1. Introduction

Effluents from industries such as food, paper, dye-stuffs, plastics, and textiles generate considerable amount of color due to dyes [1]. It is recognized that public perception of water quality is greatly influenced by the color. The presence of very small amounts of dyes (even less than 1 ppm for some dyes)

in water is highly visible and aesthetically unpleasant [2–5]. Furthermore, coloration of water by dyes may affect photochemical activities of the aquatic system by reducing light penetration [6–9].

Due to their good solubility, dyes are common water pollutants and they may frequently be found in trace quantities in industrial wastewater. Many of these dyes are also toxic and even carcinogenic, and this poses a serious hazard to aquatic living organisms

---

\*Corresponding author.

[10–13]. Methylene blue (MB) is a heterocyclic aromatic chemical compound, which has many uses in a range of different fields, like biology and chemistry. At doses of 2–4 mg/kg, hemolytic anemia and skin desquamation may occur in infants. At doses of 7 mg/kg, nausea, vomiting, chest pain, fever, and hemolysis have been described. Hypotension may occur at doses of 20 mg/kg, and bluish discoloration of the skin can occur at 80 mg/kg [2]. While methyl violet (MV) is an organic compound that is mainly used as purple dye for textiles and to give deep violet colors in paint and ink. MV is a mutagen and mitotic poison, therefore concerns exist regarding the ecological impact of the release of MV into the environment [1,2].

There are several methods used for treatment of dye containing wastewater, including reverse osmosis [14], chemical oxidation [15], photodegradation [16], electrocoagulation–electroflotation [17], and adsorption [4–13,18]. Among these methods, adsorption had become superior to other techniques for wastewater treatment in terms of low initial cost, simplicity of design, and ease of operation. In general, the activated carbon is used to absorptive removal of dyes from wastewater [19–22]. However, regeneration and reuse of activated carbon make it more costly. Therefore, it is necessary to study the feasibility of using low cost substances as adsorbents [23].

Camellia seed powder (CSP) is a granulated waste by-product from tea oil production in south provinces in China. About 2,000 tons of CSP is processed per annum just in a county of Guangxi Zhuang Autonomous Region of China. Nowadays, CSP is usually abandoned or burnt in the open air, not only releasing large amount of hazardous particles, but also polluting the environment. Therefore, the utilization of CSP is important to environmental protection and the comprehensive usage of forestry resources. Within this paper, the CSP is used as adsorbent for the first time, to remove dyes from polluted water, and the corresponding adsorption kinetic, equilibrium, and thermodynamic studies were carried out.

## 2. Materials and methods

### 2.1. Adsorbent

CSP was purchased from Beijing Boyangxin Technology Company Limited, with mesh size less than 0.59 mm. Before usage, the CSP was decolorized with water and was dried under room temperature. The surface morphology of the adsorbent was studied by an S-4800 scanning electron microscope (SEM) (Hitachi, Japan) at an accelerating voltage of 1.0 kV. Surface area and pore analysis of the adsorbent were measured by

nitrogen adsorption and desorption at 77 K using a TriStar II surface area and porosity analyzer (Micromeritics Instrument Corporation).

### 2.2. Adsorbate

Two cationic dyes, MB (Sinopharm Chemical Reagent Co., Ltd. Shanghai, China) with molecular formula of  $C_{16}H_{18}N_3SCl$  (FW 319.85 g/mol) and MV (Sinopharm Chemical Reagent Co., Ltd. Shanghai, China) with molecular formula of  $C_{25}H_{30}N_3Cl$  (FW 408.03 g/mol) were chosen as the adsorbates. The molecular structures of MB and MV are illustrated in Fig. 1. The MB and MV were chosen in this study because of their known strong adsorption onto solids. The dye stock solutions were prepared by dissolving accurately weighted MB and MV in ultra-pure water to the concentration of 100 mg/L. The experimental solutions were obtained by diluting the stock solution in accurate proportions to the required initial concentrations.

### 2.3. Adsorption equilibrium experiments

One liter solutions of MB with initial concentration of 60, 80, and 100 mg/L and solutions of MV with initial concentration of 10, 30, and 50 mg/L were treated with 6, 8, 10 g/L of CSP, respectively. The mixtures were vibrated in *constant temperature water bath oscillator with* speed of 150 r/min at different temperatures (298, 303, 308, 313, and 318 K). Three milliliter of the suspension was taken out using 0.2  $\mu$ m syringe filter (Tianjin Jinteng) every given time interval, and the filtrates were analyzed for the residual MB and MV concentration by Shimadzu UV–visible spectrophotometer (UV-1240) at 662 and 583 nm, respectively. The amount of MB and MV uptake and the removal percentage by CSP in each flask was calculated using Eqs. (1) and (2).

$$q = \frac{(C_0 - C_e)V}{W} \quad (1)$$

$$\eta = \frac{(C_0 - C_e)}{C_0} \times 100\% \quad (2)$$

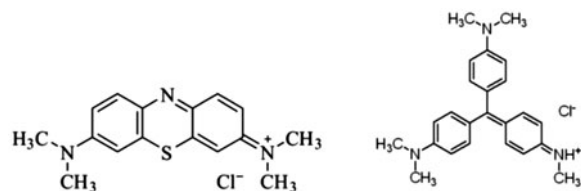


Fig. 1. Molecular structure of MB (left) and MV (right).

where  $q$  is the amount of dye adsorbed by CSP (mg/g),  $C_0$  and  $C_e$  are the initial and final dye concentrations (mg/L), respectively.  $V$  is the volume of the solution (L),  $W$  is the adsorbent weight (g), and  $\eta$  is the removal percentage of dye from the solution.

#### 2.4. Effect of pH

In order to investigate the effect of pH on MB and MV adsorption, 8.0 and 6.0 g of CSPs were added to 1.0 L solutions containing 80 mg/L of MB and 50 mg/L of MV, respectively. The initial pH values were adjusted to 3.0, 4.0, 5.0, 6.0, and 7.0 for MB system, and 3.5, 4.5, 5.5, 6.5, and 7.5 for MV system, using HCl and NaOH solutions with suitable concentration. The suspensions were filtered through 0.2  $\mu$ m syringe filter and analyzed for residual MB and MV concentration.

### 3. Results and discussion

#### 3.1. Characterization of CSP

Fig. 2 shows the SEM micrograph of a typical CSP sample at 10,000  $\times$  magnification. The CSP particles were mostly irregular in shape and were porous. The surface area of CSP as calculated by the BET method was found to be 128.7 m<sup>2</sup>/g; and the total pore volume is 0.0261 cm<sup>3</sup>/g.

#### 3.2. Effect of pH on the adsorption amount and removal percentage

The pH of solution is one of the most important parameters affecting the adsorption capacity of absor-

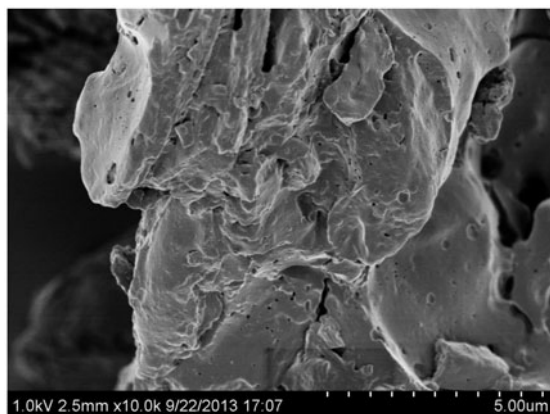


Fig. 2. SEM image of CSP.

bents [15,16]. The dependence of pH on the adsorption of two cationic dyes onto CSP is illustrated in Fig. 3. The adsorption amount of MB and MV by CSP increases slightly with pH. It is evident that the adsorption behavior of each cationic dye is similar from pH 3.0–7.5. The pH of original CSP solution is ca. 5.5; and at this pH value, the adsorption amounts of MB and MV are 9.62 and 8.17 mg/g, respectively. Therefore, in this study, the pH was unadjusted during the adsorption of MB and MV.

#### 3.3. Adsorption kinetics

Figs. 4 and 5 show the effects of contact time on the adsorption amount and removal percentage of MB and MV by CSP. The adsorption amount ( $q$ ) and removal rate ( $\eta$ ) of MB and MV by CSP were found to increase with the increase in contact time, and the maximum values were reached after 30 min. And the removal rate rises with increasing CSP amount and the decreasing of initial concentration of MB and MV, which may be due to the increasing of the active adsorption sites. In fact, the less of the initial concentration of MB and MV means the larger ratio of MB and MV molecules absorbed by CSP and total MB and MV molecules. For MB and MV, the increase of the adsorption amounts and removal rates after 30 and 15 min are not significant, and hence it is fixed as the optimum contact time. The color of MB and MV in aqueous solution cannot be detected by naked eye after 30 and 15 min, respectively. Similar results have been reported in some similar references for the removal of dyes [24,25].

Kinetic studies are important in order to evaluate in order to evaluate the mechanism and efficiency of sorption process. In order to investigate the sorption kinetic of MB and MV onto CSP, pseudo-first-order, pseudo-second-order, and intra-particle diffusion kinetic models were used.

The pseudo-first-order model can be expressed as follows:

$$\ln(q_e - q_t) = \ln(q_e) - k_1 t \quad (3)$$

where  $q_t$  (mg/g) and  $q_e$  (mg/g) represent the amount of adsorbates adsorbed at  $t$  and at equilibrium time, respectively.  $k_1$  (min<sup>-1</sup>) represents the adsorption rate constant which is calculated from the plot of  $\ln(q_e - q_t)$  against  $t$ .

Pseudo-second-order model is one of the most widely used kinetic models to predict the relationship between  $q_{\text{exp}}$  and  $q_{\text{predict}}$ , which can be expressed as Eq. (4):

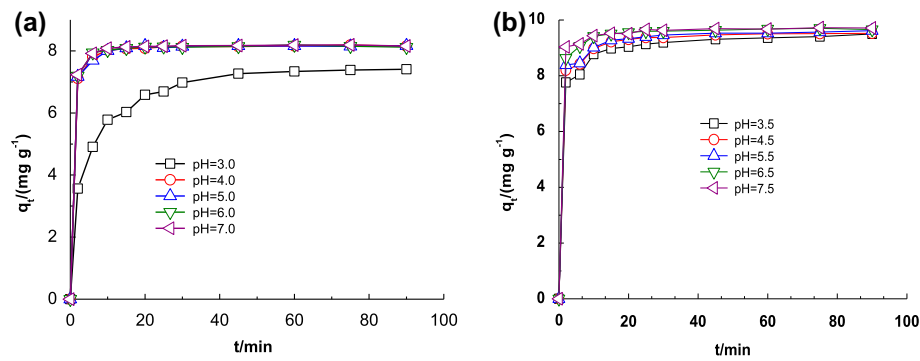


Fig. 3. Effect of different pH value on the adsorption amount of MB (a) and MV (b).

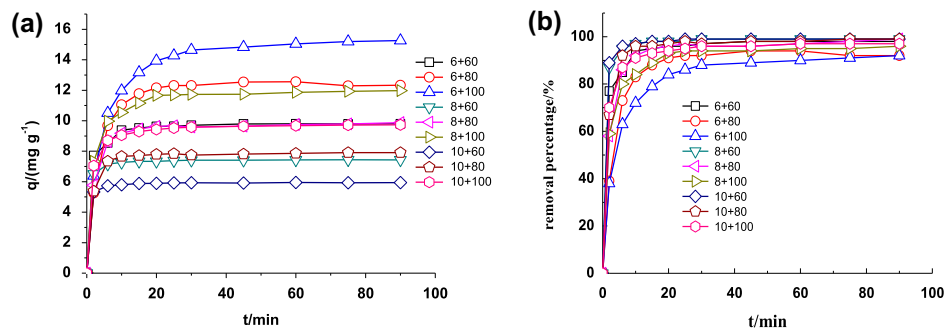


Fig. 4. Effect of different initial concentration of MB and CSP on the adsorption amount (a) and removal percentage (b).

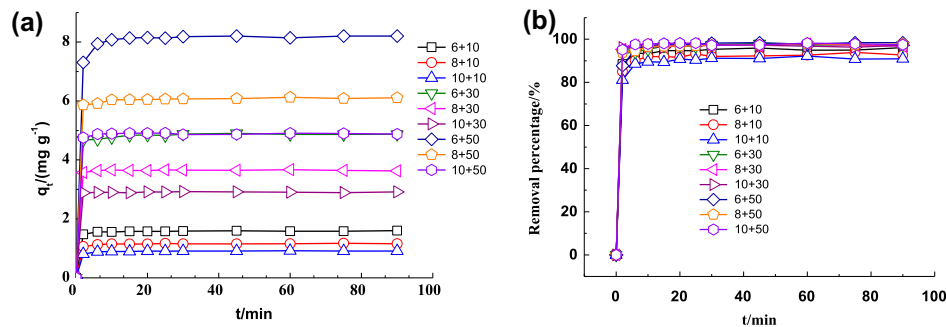


Fig. 5. Effect of different initial concentration of MV and CSP on the adsorption amount (a) and removal percentage (b).

$$\frac{t}{q_t} = \frac{1}{k_2 q_e^2} + \frac{1}{q_e} t \quad (4)$$

where  $k_2$  (g/(mg min)) is the pseudo-second-order rate constant of sorption. The plot of  $t/q_t$  vs.  $t$  should exhibit a linear relationship, and the  $q_e$  and  $k_2$  can be obtained from the slope and intercept of the plot, respectively.

Pseudo-first-order and pseudo-second-order models were used to investigate the adsorption kinetics of MB

and MV adsorption by CSP. The best model was selected depending on the linear regression correlation coefficient,  $R^2$ . As illustrated in Figs. 6 and 7 and Table 1, the pseudo-second-order model are suitable for the adsorption of MB and MV by CSP because of their relatively high  $R^2$  values, and the experimental data fit well with the pseudo-second-order model with  $R^2 > 0.99$ . The calculated  $q_e$  values (9.940 and 8.210 mg/g for MB and MV, respectively) from pseudo-second-order model are consistent with the experimental values (9.873 and 8.202 mg/g for MB and MV, respectively).

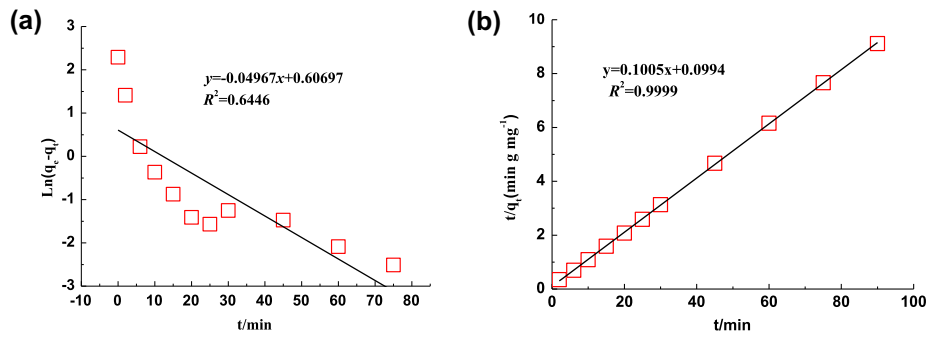


Fig. 6. Pseudo-order kinetics equation fitting curve of MB sorption onto CSP (a) pseudo-first-order kinetics; (b) pseudo-second-order kinetics.

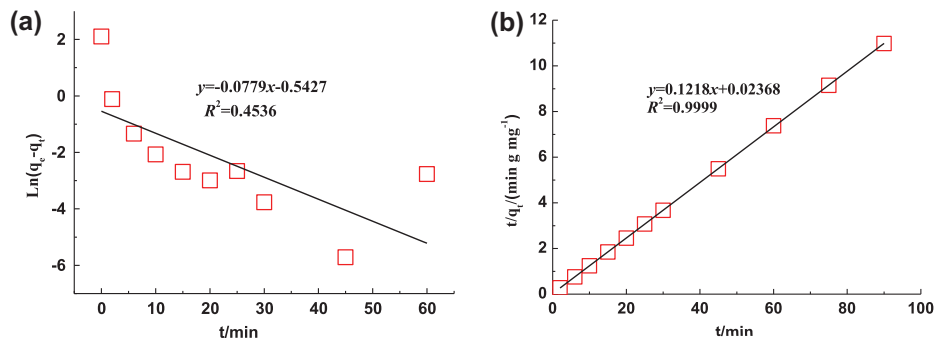


Fig. 7. Pseudo-order kinetics equation fitting curve of MV sorption onto CSP (a) pseudo-first-order kinetics; (b) pseudo-second-order kinetics.

Table 1  
Parameters of kinetic model of MB and MV adsorption onto CSP

$c_0$ (mg/L)	Dye (g/L)	Pseudo-first-order			Pseudo-second-order			Experimental value of $q_e$ (mg/g)
		$K_1$ (min <sup>-1</sup> )	$q_e$ (mg/g)	$R^2$	$K_2$ (g/mg min <sup>-1</sup> )	$q_e$ (mg/g)	$R^2$	
60	MB(8)	-0.103	0.990	0.8109	0.134	7.463	1.0000	7.435
80		-0.050	1.835	0.6446	0.101	9.900	0.9999	9.873
100		-0.061	2.988	0.8010	0.082	12.20	0.9999	11.976
10	MV(6)	-0.039	0.093	0.3007	0.626	1.597	0.9999	1.601
30		-0.074	0.346	0.6339	0.122	8.210	0.9999	8.203
50		-0.078	0.581	0.4536	0.123	8.211	0.9999	8.202

In adsorption process of dye on the solid surface, the dye species migrate towards the surface of the adsorbent. This type of migration proceeds till the existence of concentration gradient of the adsorbate species in the bulk of the solution to the surface of the adsorbent. Once equilibrium is attained, the migration of the solute species from the solution stops. The rate of an adsorption process is controlled either by external diffusion, internal diffusion, or by both types of diffusions. And the most commonly used technique

for identifying the mechanism involved in the adsorption process is using intra-particle diffusion model as Eq. (5):

$$Q = K_d t^{1/2} + I \tag{5}$$

where  $K_d$  is the intra-particle diffusion rate constant. If intra-particle diffusion occurs, then  $q$  against  $t^{1/2}$  will be linear and the line will pass through the origin, if

the intra-particle diffusion was the only rate limiting parameter controlling the process. Otherwise, some other mechanism is also involved. However, in this study, the linear plots of MB adsorption onto CSP at each concentration did not pass through the origin, and shows two linear portions (as shown in Fig. 8), in which the first part of curve (0–16 min) is attributed to boundary layer diffusion, and the final linear parts (16–90 min) indicate effect of intra-particle diffusion. While for MV adsorption onto CSP, the linear plots indicate that the effect of intra-particle diffusion plays an important role (Fig. 9). Values of  $I$  give an idea about the thickness of the boundary layer (as listed in Table 1). The  $K_d$  values increased from 0.334 to 1.534  $\text{mg}(\text{g min}^{1/2})$  for MB and 1.043 to 5.169  $\text{mg}(\text{g min}^{1/2})$  for MV, indicating that intra-particle diffusion controls the adsorption rate [26]. Simultaneously, external mass transfer resistance cannot be neglected although this resistance is only significant for the initial period of the time [27].

### 3.4. Adsorption isotherms

Adsorption isotherms describe the amount of adsorbate adsorbed and remained in the equilibrium solution at a fixed temperature. Adsorption isotherm's parameters obtained from the different models provide important information on the surface properties of the adsorbent and its affinity to the adsorbate. Several isotherm equations have been developed and employed for such analysis, and the important isotherms Langmuir, Freundlich, and Dubinin–Radushevich (D–R) isotherms are applied in this study.

The Langmuir equation is based on the assumption that the adsorption sites at the interface of the

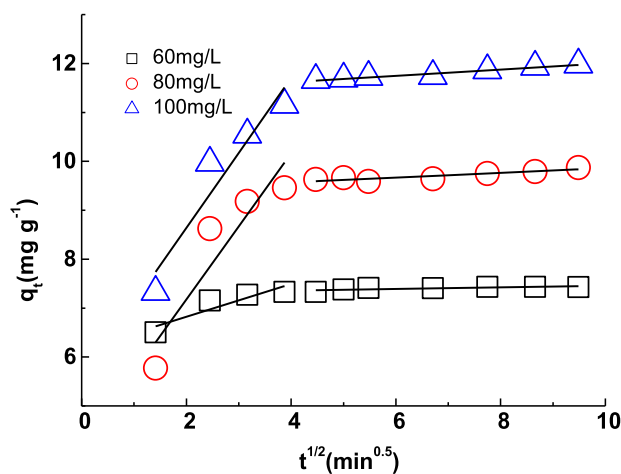


Fig. 8. Intra-particle diffusion plots for MB adsorption on CSP.

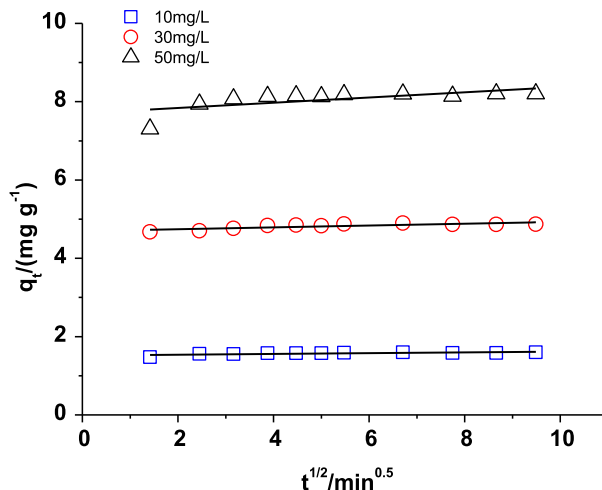


Fig. 9. Intra-particle diffusion plots for MV adsorption on CSP.

adsorbent are occupied by the adsorbate [28]. It is used to estimate the maximum adsorption capacity of the adsorbent corresponding to the complete monolayer coverage of the adsorbate on the adsorbent surface. The Langmuir isotherm is generally expressed by:

$$C_e/q_e = (1/b)q_0 + C_e/q_0 \quad (6)$$

where  $q_0$  is the maximum adsorption capacity ( $\text{mg/g}$ ) of adsorbent,  $b$  is related to the energy of adsorption which indicates the intensity of adsorption ( $\text{L/mg}$ ); high  $b$  values mean strong bonding between the adsorbate and adsorbent. The constants  $q_0$  and  $b$  can be calculated from slope and intercept of the plot, and the parameter values are listed in Tables 2 and 3.

For MB and MV in this study, the Langmuir maximum capacities of CSP were found to be 9.05 and 3.08  $\text{mg/g}$ , (as listed in Tables 2 and 3). The Langmuir isotherm has generated a satisfactory fit to the experimental data as indicated by correction coefficient. This may be due to homogeneous distribution of active sites on the CSP surface, since the Langmuir equation assumes that the surface is homogeneous [28]. The monolayer formation for the present system has been confirmed by linear plot (Figs. 10 and 11).

The shape of the Langmuir isotherm was investigated by the dimensionless constant separation term ( $R_L$ ) to determine high affinity adsorption [29,30].  $R_L$  was calculated as follows:

$$R_L = \frac{1}{1 + bC_0} \quad (7)$$

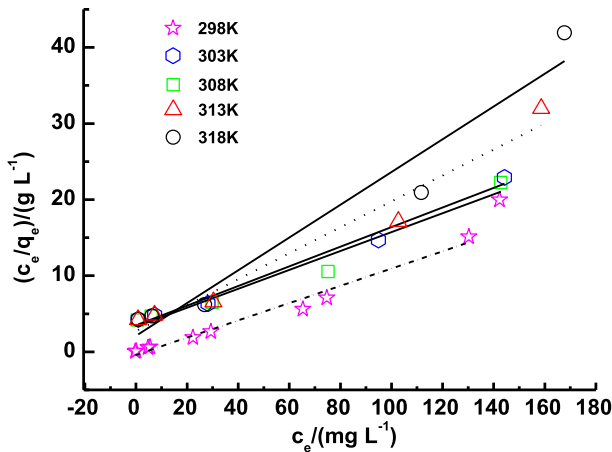


Fig. 10. Langmuir isotherms for adsorption MB by CSP.

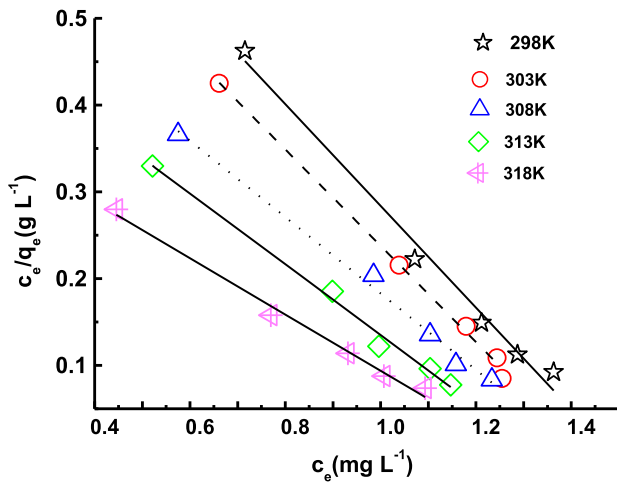


Fig. 11. Langmuir isotherms for adsorption MV by CSP.

where  $C_0$  is the initial dye concentration (mg/L).  $R_L$  indicates the type of isotherm to be irreversible ( $R_L = 0$ ), favorable ( $0 < R_L < 1$ ), linear ( $R_L = 1$ ), or unfavorable ( $R_L > 1$ ). The  $R_L$  values of MB and MV adsorbed onto CSP range from 0.045 to 0.140 and from 0.025 to 0.029,

respectively, which are between 0 and 1, indicating that both the adsorptions of MB and MV onto CSP are favorable.

The performance of the CSP in dye removal from the aqueous solution has also studied using the Freundlich isotherms [9–12,31,32]. The Freundlich isotherm is an empirical equation which assumes that the adsorption of adsorbent increases with the concentration of the adsorbate. It is used to estimate the adsorption intensity of the adsorbent towards the adsorbate. It is generally given by:

$$\log q_e = \log K_f + (1/n) \log C_e \quad (8)$$

where  $K_f$  is the amount of adsorbate that adsorbed in per unit adsorbate. High  $K_f$  values indicate easy uptake of the adsorbate. The slope  $1/n$  of Freundlich equation indicates the surface heterogeneity of the adsorbent, where  $1/n$  values of closer to zero is indicative of relative energy distribution on the adsorbent surface (or surface heterogeneity). As listed in Tables 2 and 3, for MB, the  $1/n$  values decrease from 0.117 to 0.014, implying that high temperature favors higher heterogeneity. While for MV, the  $1/n$  values were bigger than one, indicating the lower heterogeneity of MV onto SCP [33].

The D–R isotherm assumes that sorption has a multilayer character with heterogeneity of surface energies, involves van der waals forces and is applicable for physical sorption process, and which is used to determine the characteristic porosity and the apparent free energy of adsorption [34–36]. The mechanism of MB and MV adsorption from solution onto CSP surface was then examined with D–R equation:

$$\log q_e = \log q_m - K_{DR} \varepsilon^2 \quad (9)$$

where  $K_{DR}$  is a constant related to the mean free energy of adsorption ( $\text{mol}^2/\text{J}^2$ ),  $q_m$  is the theoretical saturation capacity (mol/g),  $\varepsilon$  is the polanyi potential (J/mol), which is related to the equilibrium concentration  $C_e$  (mg/L) as follows:

Table 2  
Parameters of intra-particle diffusion model

$c_{MB}$ (mg/L)	$K_d$		$I$		$c_{MV}$ (mg/L)	$K_d$		$I$
	0–8 min	8–90 min	0–8 min	8–90 min		0–90 min		
60	0.334	0.016	6.155	7.293	10	0.010	1.519	
80	1.494	0.048	4.187	9.376	30	0.023	4.696	
100	1.534	0.064	5.569	11.366	50	0.069	7.706	

Table 3

Constants of Langmuir, Freundlich, and D–R isotherms for MB and MV adsorption by CSP at different temperatures

T (K)	$q_{\text{exp}}(\text{mg/g})$	Langmuir			Freundlich			D–R		
		$q_{\text{max}}(\text{mg/g})$	$K_L(\text{L/mg})$	$R^2$	$K_F(\text{L/g})$	$1/n$	$R^2$	$K_{\text{DR}}$	$E(\text{kJ/mol})$	$R^2$
MB										
298	9.05	9.19	0.266	0.9824	6.877	0.117	0.6949	0.034	3.824	0.8565
303	7.15	7.31	0.159	0.9678	6.370	0.095	0.3961	0.091	2.343	0.7331
308	6.02	6.19	0.128	0.9585	6.370	0.068	0.1648	0.149	1.835	0.5471
313	4.65	4.84	0.094	0.9346	6.645	0.027	0.0222	0.108	2.150	0.2974
318	3.57	3.75	0.077	0.9055	7.159	0.014	0.0038	0.102	2.210	0.1459
MV										
298	1.55	1.71	0.674	0.9880	4.535	3.433	0.9813	0.751	0.816	0.9492
303	1.56	1.80	0.700	0.9971	5.454	3.241	0.9509	0.629	0.892	0.9169
308	1.57	2.27	0.707	0.9750	6.790	2.813	0.9511	0.470	1.031	0.9092
313	1.58	2.45	0.751	0.9924	8.504	2.718	0.9629	0.401	1.116	0.9213
318	1.59	3.08	0.776	0.9900	10.671	2.438	0.9840	0.311	1.269	0.9451

Table 4

Thermodynamic parameters for sorption process of MB and MV on CSP at different temperatures

T/K	$K_L$ (L/mg)	$\Delta G^0$ (kJ/mol)	$\Delta S^0$ (J/mol/K)	$\Delta H^0$ (kJ/mol)
MB				
298	127,973	–29.14	–62.33	–47.47
303	76,228	–28.32		
308	61,322	–28.23		
313	45,024	–27.88		
318	37,072	–27.81		
MV				
298	322,819	–31.43	124	5.54
303	335,264	–32.05		
308	338,452	–32.60		
313	359,846	–33.29		
318	371,652	–33.91		

$$\varepsilon = RT \ln(1 + 1/C_e) \quad (10)$$

The slope of the plot of  $\ln q_e$  vs.  $\varepsilon^2$  gives  $K_{\text{DR}}$  and intercept yields the adsorption capacity  $q_m$ . The mean free energy of adsorption ( $E$ , kJ/mol) was calculated from Eq. (11):

$$E = \frac{1}{\sqrt{2K_{\text{DR}}}} \quad (11)$$

The mean free energy of adsorption is the free energy change, when 1 mol of ion is transferred to surface of the solid from infinity in the solution, which is useful to estimate the type of adsorption. If its value is below 8 kJ/mol, the adsorption type can be explained by physical adsorption. If its value ranges from 8 to

16 kJ/mol, the adsorption type is chemical ion exchange, and the value beyond 16 kJ/mol can be explained by chemical adsorption [26,27]. The  $E$  values for both MB and MV adsorption onto CSP in this study are below 8 kJ/mol, indicating that the corresponding adsorption processes are physical adsorption.

As listed in Table 3, based on the correlation coefficients ( $R^2$  values) of all the isotherms studied, it was found that, for MB, Langmuir isotherm was the most suitable isotherm for the experimental data. While for MV, Langmuir, Freundlich, and D–R isotherms are all suitable.

### 3.5. Thermodynamic parameters

The thermodynamic parameters of the adsorption were determined using Eqs. (12) and (13).

$$\Delta G^0 = -RT \ln K_L \quad (12)$$

$$\ln K_L = \frac{\Delta S^0}{R} - \frac{\Delta H^0}{RT} \quad (13)$$

where  $K_L$  is the distribution coefficient at different temperatures (298, 303, 308, 313, and 318 K) and is equal to the ratio of the equilibrium amount adsorbed ( $q_e$  in mg/g) to the equilibrium concentration ( $C_e$  in mg/L) at different temperatures.  $R$  is the gas constant. Eq. (13) was applied to calculate the standard Gibbs free energies  $\Delta G^0$  and the standard entropy  $\Delta S^0$ . The values of  $\Delta H^0$  and  $\Delta S^0$  were obtained from the slope and intercept of the linear plot of  $\log K_L$  vs.  $1/T$ , respectively, as illustrated in Table 4. For the MB adsorbed onto CSP, the negative value of  $\Delta H^0$  (–47.47 kJ/mol) implies that this



adsorption process is exothermic. The negative value of  $\Delta S^0$  ( $-62.33 \text{ J}/(\text{mol K})$ ) shows decreased randomness at the solid-solution interface during the adsorption of MB onto CSP. In general,  $\Delta G^0$  for physical adsorption is between  $-20$  and  $0 \text{ kJ}/\text{mol}$ , but it ranged from  $-80$  to  $-400 \text{ kJ}/\text{mol}$  for chemical sorption. For MB adsorbed onto CSP, the calculated  $\Delta G^0$  values varied from  $-27.81$  to  $-29.14 \text{ kJ}/\text{mol}$ , when temperature decreased from  $318$  to  $298 \text{ K}$ . According to values of  $\Delta G^0$ , the sorption process of MB onto CSP could be controlled by mainly physical sorption and partially chemical sorption. The negative values of  $\Delta G^0$  indicated that the adsorption process is feasible and spontaneous nature on the adsorbent [3–7,34–36].

For the MV adsorbed onto CSP, the positive value of  $\Delta H^0$  confirmed the adsorption process is endothermic. Generally, a high  $\Delta H^0$  value may show chemisorptions ( $40$ – $120 \text{ kJ}/\text{mol}$ ) rather than physisorptions ( $<40 \text{ kJ}/\text{mol}$ ). The  $\Delta H^0$  value of MV adsorption onto CSP in this experiment was  $5.54 \text{ kJ}/\text{mol}$ , implying the adsorption process was physisorption process. And the positive value of  $\Delta S^0$  revealed the increased randomness at the solid-solution interface. The calculated  $\Delta G^0$  values varied from  $-31.43$  to  $-33.91 \text{ kJ}/\text{mol}$ , when temperature decreased from  $318 \text{ K}$  to  $298 \text{ K}$ . Based on the values of  $\Delta G^0$ , the spontaneous sorption process of MV onto CSP may be controlled by mainly physical sorption and partially chemical sorption [23,37–39].

#### 4. Conclusion

Equilibrium and kinetic studies were performed for the adsorption of MB and MV, two cationic dyes, from its aqueous solutions by CSP. The results reveal that the adsorption processes are exothermic and endothermic for MB and MV, respectively, based on their corresponding  $\Delta H^0$  values. Both adsorption processes for MB and MV onto CSP are spontaneous because their  $\Delta G^0$  values are below zero. And these two sorption processes could be mainly controlled by physical sorption. The equilibrium data have been analyzed against Langmuir, Freundlich, and D–R models; for MB, adsorption equilibrium data fitted well to Langmuir isotherms, and for MV its adsorption data fitted well to all three models. Logistic models agree very well with dynamic behavior for the kinetic sorption data when compared to pseudo-second-order kinetic model.

#### Acknowledgments

The study was financially supported by Major Science & Technology Program for Water Pollution Control and Treatment (2010ZX07320-002), Open

Research Fund Program of Key Laboratory of Urban Stormwater System and Water Environment (Ministry of Education), Beijing University of Civil Engineering and Architecture (Grant No. YH201101003), the Importation & Development of High-Caliber Talents Project of Beijing Municipal Institutions, Beijing Natural Science Foundation Program, and Scientific Research Key Program of Beijing Municipal Commission of Education, and the Training Program foundation for the Beijing Municipal Excellent Talents.

#### References

- [1] C. O'Neill, F.R. Hawkes<sup>1</sup>, D.L. Hawkes, N.D. Lourenço, H.M. Pinheiro, W. Delée, Colour in textile effluents-sources, measurement, discharge consents and simulation: A review, *J. Chem. Technol. Biotechnol.* 74 (1999) 1009–1018.
- [2] T. Robinson, G. McMullan, R. Marchant, P. Nigam, Remediation of dyes in textile effluent: A critical review on current treatment technologies with a proposed alternative, *Bioresour. Technol.* 77 (2001) 247–255.
- [3] J. Mittal, V. Thakur, H. Vardhan, A. Mittal, Batch removal of hazardous Azo Dye Bismark Brown R using waste material hen feather, *Ecol. Eng.* 60 (2013) 249–253.
- [4] A. Mittal, D. Jhare, J. Mittal, Adsorption of hazardous dye Eosin Yellow from aqueous solution onto waste material De-oiled Soya: Isotherm, kinetics and bulk removal, *J. Mol. Liq.* 179 (2013) 133–140.
- [5] A. Mittal, V. Thakur, V. Gajbe, Adsorptive removal of toxic azo dye Amido Black 10B by hen feather, *Environ. Sci. Pollut. Res.* 20 (2013) 260–269.
- [6] G. Crini, Non-conventional low-cost adsorbents for dye removal: A review, *Bioresour. Technol.* 97 (2006) 1061–1085.
- [7] A. Mittal, D. Jhare, J. Mittal, V.K. Gupta, Batch and bulk removal of hazardous colouring agent rose Bengal by adsorption over bottom ash, *RSC Adv.* 2(22) (2012) 8381–8389.
- [8] A. Mittal, V. Thakur, V. Gajbe, Evaluation of adsorption characteristics of an anionic azo dye Brilliant Yellow onto hen feathers in aqueous solutions, *Environ. Sci. Pollut. Res.* 19 (2012) 2438–2447.
- [9] A. Mittal, V.K. Gupta, Adsorptive removal and recovery of azo dye Eriochrome Black T., *Toxicol. Environ. Chem.* 92 (2010) 1813–1823.
- [10] M. Qiu, C. Qian, J. Xu, J. Wu, G. Wang, Studies on the adsorption of dyes into clinoptilolite, *Desalination* 243 (2009) 286–292.
- [11] H. Daraei, A. Mittal, M. Noorisepheer, J. Mittal, Separation of chromium from water samples using egg shell powder as a low-cost sorbent: Kinetic and thermodynamic studies, *Desalin. Water Treat.* doi: [10.1080/19443994.2013.837011](https://doi.org/10.1080/19443994.2013.837011).
- [12] J. Mittal, D. Jhare, H. Vardhan, A. Mittal, Utilization of bottom ash as a low-cost sorbent for the removal and recovery of a toxic halogen containing dye Eosin Yellow, *Desalin. Water Treat.* doi: [10.1080/19443994.2013.803265](https://doi.org/10.1080/19443994.2013.803265).

- [13] A. Mittal, V. Thakur, J. Mittal, H. Vardhan, Process development for the removal of hazardous anionic azo dye Congo-Red from wastewater by using hen feather as potential adsorbent, *Desalin. Water Treat.* doi: 10.1080/19443994.2013.785030.
- [14] S.K. Nataraj, K.M. Hosamani, T.M. Aminabhavi, Nanofiltration and reverse osmosis thin film composite membrane module for the removal of dye and salts from the simulated mixtures, *Desalination* 249 (2009) 12–17.
- [15] K. Dutta, S. Mukhopadhyay, S. Bhattacharjee, B. Chaudhuri, Chemical oxidation of methylene blue using a Fenton-like reaction, *J. Hazard. Mater.* 84 (2001) 57–71.
- [16] I. Poullos, I. Tsachpinis, Photodegradation of the textile dye Reactive Black 5 in the presence of semiconducting oxides, *J. Chem. Technol. Biotechnol.* 74 (1999) 349–357.
- [17] W. Balla, A.H. Essadki, B. Gourich, A. Dassaa, H. Chenik, M. Azzi, Electrocoagulation/electroflotation of reactive, disperse and mixture dyes in an external-loop airlift reactor, *J. Hazard. Mater.* 184 (2010) 710–716.
- [18] M.A.M. Salleh, D.K. Mahmoud, W.A. Karim, A. Idris, Cationic and anionic dye adsorption by agricultural solid wastes: A comprehensive review, *Desalination* 280 (2011) 1–13.
- [19] K.Y. Foo, B.H. Hameed, An overview of dye removal via activated carbon adsorption process, *Desalin. Water Treat.* 19 (2010) 255–274.
- [20] A.A. Ahmad, A. Idris, B.H. Hameed, Organic dye adsorption on activated carbon derived from solid waste, *Desalin. Water Treat.* 51 (2013) 2554–2563.
- [21] B.H. Hameed, A.T.M. Din, A.L. Ahmad, Adsorption of methylene blue onto bamboo-based activated carbon: Kinetics and equilibrium studies, *J. Hazard. Mater.* 141 (2007) 819–825.
- [22] A.H. Sulaymon, W.M. Abood, Removal of reactive yellow dye by adsorption onto activated carbon using simulated wastewater, *Desalin. Water Treat.* 19 (2013) 1–11.
- [23] X. Chen, S. Lv, S. Liu, P. Zhang, A. Zhang, J. Sun, Y. Ye, Adsorption of methylene blue by rice hull ash, *Sep. Sci. Technol.* 47 (2012) 147–156.
- [24] S. Lagergren, About the theory of so-called adsorption of soluble substances, *Kungliga Svenska Vetenskapsakademiens Handlingar.* 24 (1898) 1–39.
- [25] Y.S. Ho, G. McKay, Sorption of dye from aqueous solution by peat, *Chem. Eng. J.* 70 (1998) 115–124.
- [26] W.J. Weber Jr., J.C. Morris, Kinetics of adsorption on carbon from solutions, *J. Sci. Eng. Div.* 89 (1963) 31–59.
- [27] I.D. Mall, V.C. Srivastava, N.K. Agarwal, Removal of Orange-G and methyl violet dyes by adsorption onto bagasse fly ash—Kinetic study and equilibrium isotherm analyses, *Dyes Pigm.* 69 (2006) 210–223.
- [28] M. Özacar, İ.A. Şengil, Adsorption of metal complex dyes from aqueous solutions by pine sawdust, *Bioresour. Technol.* 96 (2005) 791–795.
- [29] M.V. Subbaiah, Y. Vijaya, A.S. Reddy, G. Yuvaraja, A. Krishnaiah, Equilibrium, kinetic and thermodynamic studies on the biosorption of Cu(II) onto *Trametes versicolor* biomass, *Desalination* 276 (2011) 310–316.
- [30] Z.Y. Yao, J.H. Qi, L.H. Wang, Equilibrium, kinetic and thermodynamic studies on the biosorption of Cu(II) onto chestnut shell, *J. Hazard. Mater.* 174 (2010) 137–143.
- [31] R. Jain, S. Sikarwar, Removal of hazardous dye congo red from waste material, *J. Hazard. Mater.* 152 (2008) 942–948.
- [32] A. Mittal, J. Mittal, L. Kurup, Adsorption isotherms, kinetics and column operations for the removal of hazardous dye, Tartrazine from aqueous solutions using waste materials—Bottom ash and De-oiled Soya, as adsorbents, *J. Hazard. Mater.* 136 (2006) 567–578.
- [33] M.A. Al-Ghouti, M.A.M. Khraisheh, S.J. Allen, M.N. Ahmad, The removal of dyes from textile wastewater: A study of the physical characteristics and adsorption mechanisms of diatomaceous earth, *J. Environ. Manage.* 69 (2003) 229–238.
- [34] E. Eren, Removal of basic dye by modified Unye bentonite, *J. Hazard. Mater.* 162 (2009) 1355–1363.
- [35] N.K. Amin, Removal of direct blue-106 dye from aqueous solution using new activated carbons developed from pomegranate peel: Adsorption equilibrium and kinetics, *J. Hazard. Mater.* 165 (2009) 52–62.
- [36] Ö. Gerçela, H.F. Gerçelb, A.S. Kopalalc, U.B. Oğütveren, Removal of disperse dye from aqueous solution by novel adsorbent prepared from biomass plant material, *J. Hazard. Mater.* 160 (2008) 668–674.
- [37] A. Çelekli, B. Tanrıverdi, H. Bozkurt, Predictive modeling of removal of Lanaset Red G on *Chara contraria*; kinetic, equilibrium, and thermodynamic studies, *Chem. Eng. J.* 169 (2012) 166–172.
- [38] P. Senthil Kumar, S. Ramalingam, C. Senthamarai, M. Niranjanaa, P. Vijayalakshmi, S. Sivanesan, Adsorption of dye from aqueous solution by cashew nut shell: Studies on equilibrium isotherm, kinetics and thermodynamics of interactions, *Desalination* 261 (2010) 52–60.
- [39] N. Hidalgo, G. Mangiameli, T. Manzano, G.G. Zhadan, J.F. Kennedy, V.L. Shnyrov, M.G. Roig, Oxidation and removal of industrial textile dyes by a novel peroxidase extracted from post-harvest lentil (*Lens culinaris* L.) stubble, *Biotechnol. Bioprocess Eng.* 16 (2011) 821–829.